

Source Apportionment of Speciated Mercury in Chinese Rice Grain Using a High-Resolution Model

Yuying Cui,[#] Qingru Wu,[#] Kaiyun Liu, Shuxiao Wang,* Xun Wang, Tao Jiang, Bo Meng, Yurong Wu, and Jia Guo



Cite This: *ACS Environ. Au* 2022, 2, 324–335



Read Online

ACCESS |

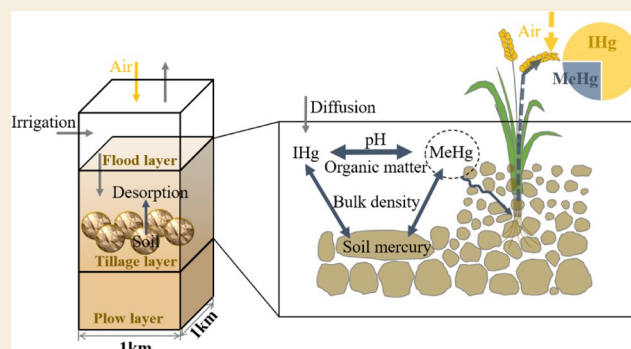
Metrics & More

Article Recommendations

Supporting Information

ABSTRACT: Rice grain consumption is a primary pathway of human mercury exposure. To trace the source of rice grain mercury in China, we developed a rice paddy mercury transport and transformation model with a grid resolution of 1 km × 1 km by using the unit cell mass conservation method. The simulated total mercury (THg) and methylmercury (MeHg) concentrations in Chinese rice grain ranged from 0.08 to 243.6 and 0.03 to 238.6 μg/kg, respectively, in 2017. Approximately, 81.3% of the national average rice grain THg concentration was due to atmospheric mercury deposition. However, soil heterogeneity, especially the variation in soil mercury, led to the wide rice grain THg distribution across grids. Approximately, 64.8% of the national average rice grain MeHg concentration was due to soil mercury. In situ methylation was increased. The coupled impact of high mercury input and methylation potential led to extremely high rice grain MeHg in partial grids among Guizhou province and junctions with surrounding provinces. The spatial variation in soil organic matter significantly impacted the methylation potential among grids, especially in Northeast China. Based on the high-resolution rice grain THg concentration, we identified 0.72% of grids as heavily polluted THg grids (rice grain THg > 20 μg/kg). These grids mainly corresponded to areas in which the human activities of nonferrous metal smelting, cement clinker production, and mercury and other metal mining were conducted. Thus, we recommended measures that are targeted at the control of heavy pollution of rice grain by THg according to the pollution sources. In addition, we observed a wide spatial variation range of MeHg to THg ratios not only in China but also in other regions of the world, which highlights the potential risk of rice intake.

KEYWORDS: mercury, methylmercury, rice paddy mercury transport and transformation model, atmospheric mercury deposition, soil mercury, source apportionment



1. INTRODUCTION

Mercury pollution poses a great threat to human health and ecological safety.^{1–3} Methylmercury (MeHg) severely affects neurodevelopment and is associated with cardiovascular disease in adults, thereby leading to long-term negative effects on human health.^{4,5} To protect human health from mercury pollution, the Minamata Convention on Mercury was put into effect in 2017, which requires the evaluation of health benefits from atmospheric mercury emission reductions. An integrated model in which emissions, chemical transport modeling, deposition to food MeHg, intelligence quotient effects, and cardiovascular impacts are considered will assist in achieving this aim.⁶ Quantifying the relationship between environmental mercury and accumulated speciated mercury in rice grain is of great significance to the development of such an integrated model.

Rice grain has a high ability to accumulate MeHg and is one of the main sources of MeHg exposure for humans globally,

especially in China.^{7–9} Observations have shown that mercury in ambient air is a potential source of inorganic mercury (IHg) above the ground.^{10,11} Isotope experiments proved that rice grain IHg comes almost entirely from air.^{12,13} Rice grain MeHg accumulates mainly from paddy soil.^{10,12,14,15} Thus, soil, irrigation water, and air are potential sources of MeHg in paddy soil.^{13,16,17} The accumulation of rice grain MeHg is a complex process that is impacted by many factors, such as bioavailable mercury, organic matter, pH, and root accumulation.^{10,12,14–16,18–21} Not all mercury in the pore water layer is involved in the methylation process. Mercury that is easily

Received: December 15, 2021

Revised: April 17, 2022

Accepted: April 18, 2022

Published: May 2, 2022



utilized by methylated microorganisms is called bioavailable mercury.¹⁶ Water-soluble mercury, organically bound mercury, iron–sulfur-bound mercury, and nanoparticulate mercuric sulfide are potentially methylated.^{16,22,23} Soil organic matter (SOM) and pH affect the content of bioavailable mercury and the activity of methylating microorganisms; organic matter also affects the adsorption and desorption of mercury.^{21,24,25} However, most previous model studies assessed rice grain MeHg concentrations according to a relatively singular pathway.^{8,26} The rice grain MeHg concentrations were scaled by the strong correlation with soil mercury concentrations in a previous study.⁸ Other studies applied a linear correlation between mercury concentrations in atmospheric deposition and rice grain MeHg^{6,26,27} under the assumption that the newly deposited atmospheric mercury had higher bioavailability and was more easily converted to MeHg.^{28,29} Due to the neglect of the impacts of many other factors, as discussed above, it is quite possible that the assumption in the model that rice grain mercury originates from a single environmental medium is of highly uncertain validity.

In reality, rice grain total mercury (THg) and MeHg concentrations show large spatial variations in China. Spatially refined models help better quantify the sources of speciated mercury in rice grain. To determine rice grain mercury sources and to identify factors that influence spatiotemporal variability in Chinese rice grain mercury concentrations, Kwon et al. (2018) constructed a rice paddy biogeochemical cycle model that considered multiple medium sources and elucidated important processes and factors that govern mercury concentrations in rice grain.³⁰ However, this model mainly simplifies the mercury reaction mechanism in soil by using a unified rate coefficient and ignoring the impact of the significant spatial heterogeneities of soil properties [mercury content, SOM, pH, etc.], which are the main sources of uncertainty in rice grain MeHg simulation. For example, studies have indicated that MeHg in rice grain is significantly correlated with SOM,^{25,31} which can vary from 0.16 to 23.7% in rice paddies across China.³²

To better quantify the sources of speciated mercury in rice grain, in this study, we developed a rice paddy mercury transport and transformation model (RMTTM) by using the unit cell mass conservation method with a spatial resolution of 1 km × 1 km. Our model mainly considers the influences of multiple-medium mercury input, high-resolution soil heterogeneity, rice grain phenological sequences, mercury transport and transformation process in rice paddies, and speciated mercury accumulation in rice grain. By using the RMTTM, we determined the spatial variations of mercury sources for China's rice grain and identified the heavily polluted regions. This model will facilitate the development of detailed mercury pollution control strategies that will reduce the health risks of mercury pollution. In addition, the model framework will aid in the development of an integrated model for evaluating the effectiveness of the Minamata Convention on Mercury.

2. METHODOLOGY

In this study, we constructed a gridded RMTTM and corresponding data set. Rice paddies were divided into 464,368 grids with a spatial resolution of 1 km × 1 km according to the distribution of paddy fields in China, which was obtained from the China Land Use and Land Cover Remote Sensing Monitoring database (Supporting Information S1 and Figure S1).^{33,34} The geographical scope of the database

was the China region, and the scope was determined using Landsat 8 remote sensing image data. The spatial resolution of soil property data, such as SOM, pH, and soil bulk density (BD) data, was 1 km × 1 km. Therefore, 1 km × 1 km was selected as the basic simulation unit in the model. In each grid, we divided the paddy soil into three layers: the flood layer, which retained overlying water (with a depth of approximately 10 cm from the atmosphere–water interface); the tillage layer, where rice roots grew (with a depth of approximately 20 cm between flood water and the plow layer, which is also called the pore water layer); and the plow layer (a relatively compact soil layer below the tillage layer). Due to the influence of wind, the disturbance of the rice plants, and the dissolution and diffusion effects of pollutants in flood water, the pollutant concentrations in flood water tend to be uniform.^{35,36} Therefore, we assumed fast mixing of mercury in the flood water layer. In the tillage layer, mercury undergoes a series of transport and transformation processes and is absorbed by the root system. We simulated the mercury behaviors based on the unit cell mass conservation method, where the product of the previous layer is used as the input of the next layer. The plow layer improves the ability of soil to retain water, as it prevents water from draining away.³⁵ Therefore, mercury in the pore water layer was assumed to be blocked by the plow layer, and the mercury exchange flux at the bottom boundary was ignored. Mercury transport and transformation generally occur in flood water and pore water, which involve atmosphere–water, water–soil, and soil–rice root interfaces and the transformation processes of multiple forms of mercury [e.g., divalent mercury (Hg^{2+}) reduction, MeHg demethylation, and Hg^{2+} methylation], as illustrated in Figure 1. Then, we established the transport and transformation mechanisms in different layers by using the unit cell mass conservation method and grid-specific parameters.

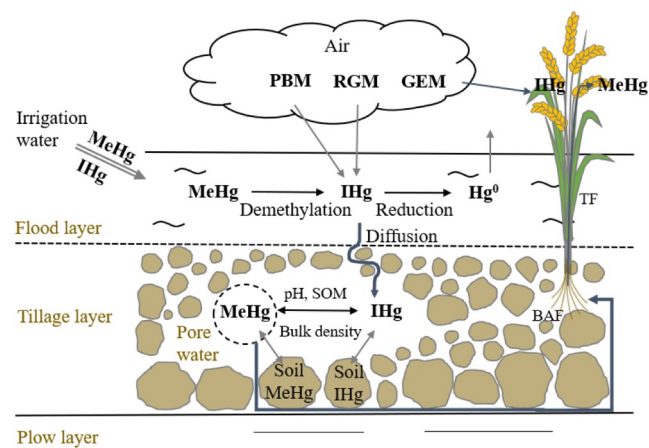


Figure 1. Mercury transport and transformation in rice paddies. [(1) Mercury input: PBM and RGM deposition into the flood water; GEM deposition into rice plants; and irrigation water input and soil mercury desorption. (2) Transport and transformation in rice paddies: demethylation and reduction in the flood water and diffusion, adsorption, methylation, and demethylation in the tillage layer. (3) Accumulation in rice grain: MeHg absorbed by roots and transported to rice grain and IHg absorbed from air. PBM: particle-bound mercury; RGM: reactive gaseous mercury; GEM: gaseous elemental mercury; MeHg: methylmercury; IHg: inorganic mercury; SOM: soil organic matter; BAF: bioaccumulation factor of roots; TF: transport factor; and LAI: leaf area index].

2.1. Construction of the RMTTM

The RMTTM consists of three parts: mercury input from various environmental media, mercury transport and transformation in the rice paddy, and speciated mercury accumulation in rice grain. Atmospheric mercury deposition, irrigation water mercury, and soil mercury were included as the main inputs of IHg and MeHg of rice grain. The transport and transformation module involves various mechanisms, such as reduction, methylation, demethylation, diffusion, and adsorption. The accumulation module of speciated mercury in rice grain includes MeHg accumulation in roots and transport to grains and IHg absorption from air. The detailed calculation methods are described in [Supporting Information S2](#).

2.1.1. Mercury Input Module. The mercury inputs into rice paddies are atmospheric mercury, irrigation water mercury, and soil mercury.^{37–39}

2.1.1.1. Atmospheric Mercury. The atmospheric mercury deposition rates were simulated by using a global atmospheric chemistry transport model (GEOS-Chem, version 11-01, <http://geos-chem.org>). Global simulation with a spatial resolution of $2^\circ \times 2.5^\circ$ was used as the initial and boundary conditions. Nested-grid simulation was used in mainland China with a spatial resolution of $0.25^\circ \times 0.3125^\circ$ (approximately 20×25 km). The model was driven by meteorological data from the GEOS forward processing system, and the highly resolved atmospheric mercury emissions in 2017 were from the China Atmospheric Mercury Emission model.^{40–42} We then outputted the deposition fluxes of gaseous elemental mercury (GEM), reactive gaseous mercury (RGM), and particle-bound mercury (PBM) from GEOS-Chem, as shown in [Supporting Information S2](#) and [Figure S2](#).

Atmospheric mercury can be deposited into flood water and rice plants. Due to bioavailability and chemical activity, RGM and PBM that were deposited into flood water were regarded as IHg,^{43,44} which included both dissolved ionic and PBM. Because newly deposited mercury accumulates on the soil surface,^{29,30,45} RGM and PBM were also assumed to be deposited onto the soil surface during the non-rice planting period. These fractions of mercury are also easily dissolved in the flood water during persistent flooding in the rice planting period. Therefore, a 1 year deposition period was adopted for the input of RGM and PBM. However, dry deposited GEM was assumed to be absorbed by the leaves of rice plants during the planting period of rice since rice plant leaves can absorb GEM from the atmosphere through their stomata.^{46,47}

2.1.1.2. Irrigation Water Mercury and Soil Mercury. Mercury in the rice paddy was also supplied from the irrigation water. The mercury concentrations in the irrigation water were assumed to be the same as those in China's surface water, which are in the range of 4.3–690 ng/L for THg and 0.11–1.0 ng/L for MeHg.⁴⁸ We chose the average values of 25.0 ng/L for THg and 0.5 ng/L for MeHg according to Yan et al. (2012) as the unified input data of the mercury concentration in the irrigation water.⁴⁸ Another source of mercury to paddies is mercury that is dissolved from soil mercury. The soil mercury was considered to be the sum of the geological background mercury and historical sedimentary mercury. The concentrations of IHg and MeHg that were dissolved into the pore water from the soil mercury were calculated by using [eqs S3 and S4](#). The soil mercury concentrations in the topsoil (0–20 cm) were obtained from the National Multi-Purpose Regional Geochemical Survey (NMPRGS) of China.^{49,50} The soil mercury concentration was

matched with the rice paddy and was gridded into a resolution of $1 \text{ km} \times 1 \text{ km}$ by using ArcGIS ([Figure S4](#)), which ranged from 3.3 to 18151.5 $\mu\text{g}/\text{kg}$.

2.1.2. Mercury Transport and Transformation in Rice Paddies. Inorganic mercury originating from deposition and irrigated water was assumed to exist as Hg^{2+} in the flood water due to the high chemical and biological activities of dissolved ionic and particulate-bound mercury. In flood water, Hg^{2+} and MeHg undergo photoreduction and photodemethylation, respectively.^{51–53} Therefore, the IHg input from atmospheric deposition and irrigation water, Hg^{2+} reduction, MeHg demethylation, and runoff was used to calculate the IHg concentration in the flood water ([eq S5](#)). Generally, the MeHg concentration in the pore water layer was higher than that in the flood water ([Table S5](#)). Therefore, MeHg input from irrigation water and the pore water layer, demethylation, and runoff was used to calculate the MeHg concentration in the flood water ([eq S6](#)). A numerical ordinary differential equation solver (ode45) in MATLAB software was used to solve these equations. Detailed information on the key parameters for [eq S6](#) is presented in [Table S4](#).

IHg in the flood water acted as the upper boundary concentration and diffused to the pore water layer. The movement of IHg in the pore water layer included diffusion, adsorption, methylation, and demethylation. The unit cell mass conservation method was used to describe this process. Taking an equilibrium unit at the tillage layer, the difference in IHg mass in and out of the unit was equal to the increase in IHg mass in the unit. Considering the mass conservation between the mass produced by diffusion, source input, adsorption, and chemical reaction in a short time (dt) and the mass change in the unit, a differential equation was established, and the deformation of the pore water layer was ignored to obtain [eqs 1 and 2](#). The IHg concentrations in the pore water layer were calculated by the implicit finite difference method. The mercury concentrations in rice were calculated on a monthly basis. The initial IHg concentration in the pore water was assumed to be zero. IHg diffusion (represented by D_I) calculations utilized diffusion rates for IHg which ranged from 157.7 to 409.9 cm^2/yr .^{54–56} The average value of 283.8 cm^2/yr was used as the unified input of D_I . The adsorption process was represented by the soil–water partition coefficient (K_d). The soil–water partition coefficient was defined as the concentration ratio between the solid and liquid phases and was a function of dissolved organic matter (represented by DOC) ($K_d = 1.76 \times 10^3 \times \text{DOC}^{-1}$,⁴⁹ $R^2 = 0.96$).⁵⁷

The MeHg in the pore water was mainly from the methylation of IHg and MeHg that was desorbed by the soil MeHg solution ([eq 3](#)). The methylation process in pore water is affected by many factors, such as microbiology, the available mercury content, pH, redox potential (Eh), SOM, iron, and sulfur.^{16,19,23} The methylation rate of IHg in the pore water layer was measured in the range of 0.012–40 yr^{-1} .⁵⁸ The average value of 0.073 yr^{-1} from Zhao (2016)⁵⁸ was used as the unified input of k_m , which was used in the calculation of the IHg concentration. Du et al. (2019) found that methylation efficiency (f_m) was significantly correlated with the in situ soil pH and SOM. They predicted the methylation efficiency using a regression equation of f_m with pH, SOM, and flooding time ([eq 4](#), $R^2 = 0.683$, $p < 0.0001$).⁵⁹ In our model, we applied the mercury methylation efficiency and the regression equation to acquire MeHg concentrations from the methylation of IHg. It was noted that only bioavailable IHg (represented as C_{PIem})

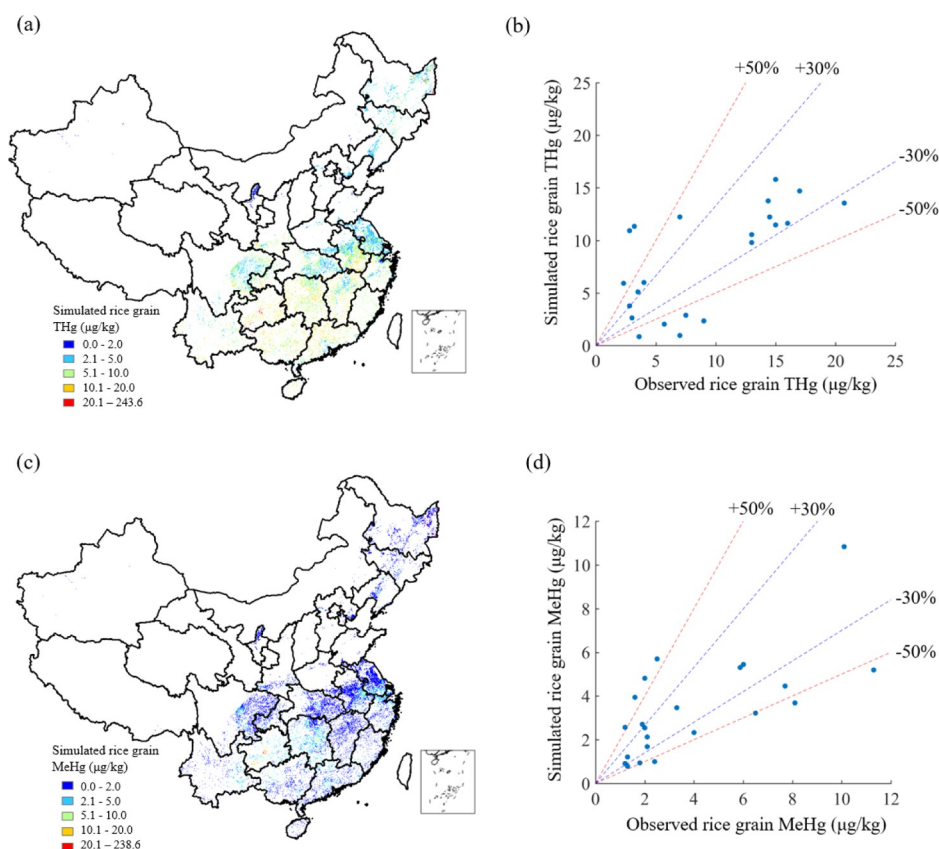


Figure 2. Simulated mercury concentrations in the rice grain and model validation. (a) Simulated THg concentrations in the rice grain at $1 \text{ km} \times 1 \text{ km}$ grids; (b) comparison between the simulated and observed THg concentrations in the rice grain; (c) simulated MeHg concentrations in the rice grain using $1 \text{ km} \times 1 \text{ km}$ grids; and (d) comparison between the simulated and observed MeHg concentrations in the rice grain. The red lines and blue lines in panels B and D represent the uncertainty ranges of $\pm 50\%$ and $\pm 30\%$, respectively.

was easily methylated. The bioavailable IHg concentration was calculated by using eq S7. Data on the pH, SOM, and BD with a resolution of $1 \text{ km} \times 1 \text{ km}$ were obtained from the soil database of China for land surface modeling.³² ArcGIS was used to match these data with the unit cell.

$$\text{IHg: } R_d \frac{\partial C_{\text{PI}}}{\partial t} = \frac{\partial}{\partial Z} \left(D_1 \frac{\partial C_{\text{PI}}}{\partial Z} \right) - k_m R_d C_{\text{PI}} + \frac{I_1}{n} \quad (1)$$

$$R_d = 1 + \frac{\text{BD}}{n} \times K_d \quad (2)$$

$$\text{MeHg: } C_{\text{PM}} = f_m \times C_{\text{PIem}} + I_m \quad (3)$$

$$\log f_m = (-1.98 - 0.025\text{pH} + 0.228\log \text{SOM}) \times t^{0.204} + 0.913 \ln t \quad (4)$$

where C_{PI} is the IHg concentration in the pore water, $\mu\text{g}/\text{m}^3$. D_1 is the diffusion coefficient of IHg, cm^2/yr . k_m is the methylation rate in the pore water layer, yr^{-1} . D_1 and k_m are described in detail in Table S4. I_1 is the dissolved soil IHg in the pore water, $\mu\text{g}/\text{m}^3$. n is the porosity of the pore water layer. R_d is the retention factor. C_{PM} is the MeHg concentration in the pore water layer, $\mu\text{g}/\text{m}^3$. f_m is the proportion of MeHg to IHg in the pore water layer, which was calculated following Du et al. (2019).⁵⁹ C_{PIem} is the bioavailable IHg concentration in the pore water layer, $\mu\text{g}/\text{m}^3$. I_m is the MeHg concentration that was dissolved from soil mercury in the pore water layer, $\mu\text{g}/\text{m}^3$; the calculation is presented in eq S4. BD is the soil bulk

density, g/cm^3 . K_d is the adsorption and desorption constant, L/kg . SOM is the concentration of soil organic matter, mg/kg . t is the rice planting time in days.

2.1.3. Mercury Accumulation in Rice Grain. MeHg and IHg in pore water are absorbed by roots and transported to rice grains for accumulation.^{12–14} Experiments have indicated that MeHg in rice grain originates from soil MeHg.^{13,14,60} Thus, we considered MeHg accumulation only in rice grains since they are the edible parts. We identified positive correlations of MeHg concentrations between roots and soil (Figure S5a, $y = 2.37x$, $R^2 = 0.88$) and between rice roots and grains (Figure S5b, $y = 3.03x$, $R^2 = 0.97$). Soil MeHg includes MeHg in the pore water and undissolved MeHg in the soil. Thus, we calculated the rice root MeHg concentration from the MeHg concentrations in the pore water and undissolved MeHg in the soil. Then, we calculated the rice grain MeHg concentration based on the above-mentioned two equations (eqs S10–S12). Additional details can be found in Supporting Information S2.3.

Rice grain can absorb GEM through the stomata and store it as IHg.^{10,11,13} The absorption and assimilation coefficient (represented by K_{ass}) was used to represent the amount of atmospheric mercury which was actually absorbed by leaves, which was related to the properties of the leaves.⁴³ During the planting period of rice, the amount of mercury which leaves absorbed from the atmosphere depended on the leaf area index (LAI) and planting time. Our research summarized the planting time series of single- and double-cropping rice in each planting period (Table S1). Data on LAI were obtained

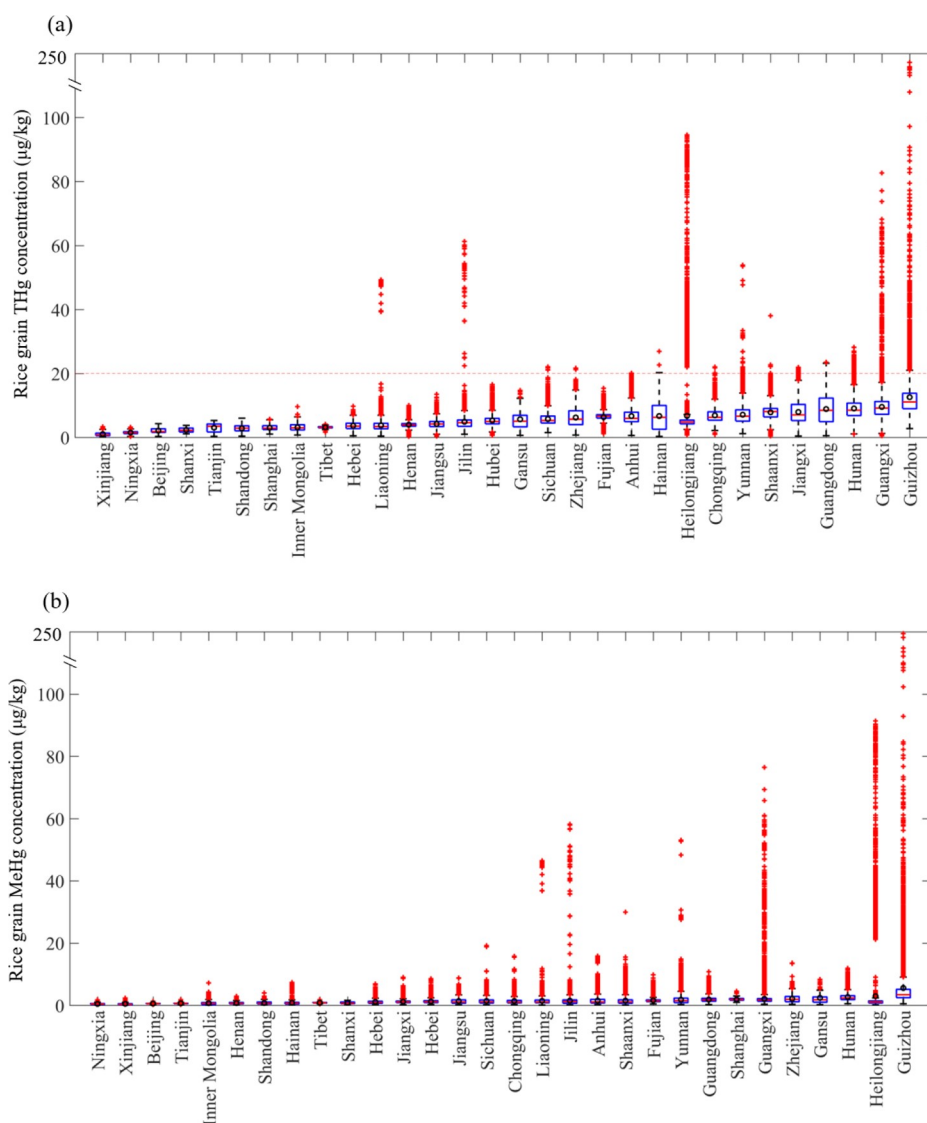


Figure 3. Provincial distribution characteristics of rice grain (a) THg and (b) MeHg. (Note: the black circles, red lines, and red crosses represent the average, median, and singular values, respectively).

from reprocessed MODIS data.⁶¹ According to data from the literature, the IHg concentrations in rice grains and leaves had a significant positive correlation (Figure S6, $y = 0.91x$, $R^2 = 0.99$), and the slope was used as the migration coefficient of IHg in leaves and rice grains. Therefore, we calculated the concentration of IHg in rice grains using the migration coefficient and the absorption and assimilation coefficient (eqs S13 and S14), as described in Supporting Information S2.3.

2.2. Model Validation

The simulation results, including the THg and MeHg concentrations in the flood water, pore water, and rice grains, were compared with observations (see Table S5 in the Supporting Information). The range of the observations was generally within the range of the simulation results, except for the maximum MeHg concentration in the flood water. The low simulated MeHg concentration in the flood water was attributed to the effect of demethylation, which was less frequently measured in rice paddies and had a large uncertainty range. The demethylation rate that was used in the model was from lakes and rivers, which had higher light-use efficiency than rice paddies.

We compared and verified the simulated concentrations of rice grain THg and MeHg (Figure 2) with the experimental data in the literature.^{62–68} Overall, the model was reliable. The normalized mean bias (NMB) and normalized mean error (NME) were used to evaluate the overall simulation effect of multiple points (Supporting Information S2.2.4). The NMB and NME of rice grain THg were -9.8 and 40.3% , respectively. For low rice grain THg concentrations (e.g., less than $10 \mu\text{g}/\text{kg}$), the simulations and observations were relatively scattered. For high concentrations of rice grain THg (e.g., higher than $10 \mu\text{g}/\text{kg}$), the simulated and calibrated values at approximately 66.7% of points were within the 30% uncertainty range, which showed better calibration results. The NMB and NME of rice grain MeHg were -13.3 and 41.6% , respectively. The calibration results of rice grain MeHg were relatively scattered; however, the simulated and observed values for most sites were still within the 50% uncertainty range.

2.3. Sensitivity Analysis

Sensitivity analyses were conducted to assess the influence of key parameters on the rice grain MeHg concentration. Figure S7 shows the results of the sensitivity analyses. They were

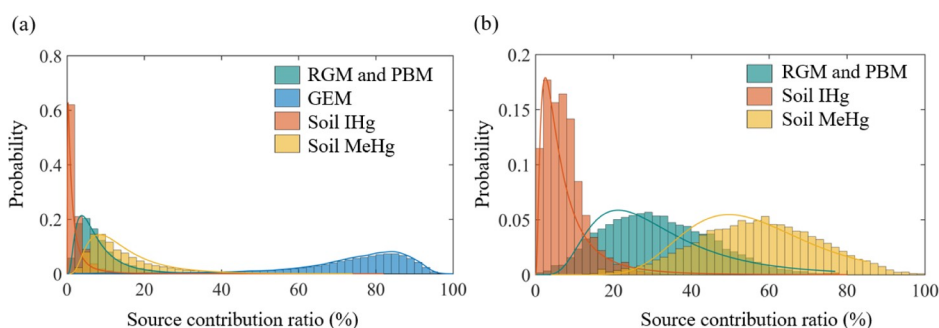


Figure 4. Source contributions to rice grain mercury concentrations. (a) THg and (b) MeHg.

based on uncertainty ranges from the literature or $\pm 10\%$ perturbations, which we called an uncertain scenario. The average rice grain MeHg concentration difference between the uncertain scenario and the base scenario that was described in Sections 2.1 and 2.2 was calculated to reflect the sensitivity. It was found that the methylation rate in the pore water had the greatest influence on the rice grain MeHg concentrations and was within the range of -0.60 to $0.08 \mu\text{g}/\text{kg}$ (Figure S7a). Similarly, other factors that may have contributed to the decrease in rice grain MeHg were the runoff rate and reduction rate in the flood water, and the ranges of decline were -0.31 and $-0.14 \mu\text{g}/\text{kg}$, respectively. We also analyzed the influence by forcing $\pm 10\%$ changes to assess the average difference and found that the runoff rate and reduction rate had greater effects on the rice grain MeHg concentration, as shown in Figure S7b. The rice grain MeHg concentration was more sensitive to the reduction and runoff rates in the flood water. The reduction of Hg^{2+} and the effect of surface runoff reduced the content of bioavailable IHg, which, in turn, reduced the content of MeHg that could be absorbed by rice plants.

3. RESULTS AND DISCUSSION

3.1. Concentrations and Source Apportionment of THg in Rice Grain

The rice grain THg concentrations in China presented a lognormal distribution with a median of $5.65 \mu\text{g}/\text{kg}$ and varied between 0.08 and $243.6 \mu\text{g}/\text{kg}$ (Figure S8a). The distribution of rice grain THg among provinces is shown in Figure 3a. The top 10 provinces with relatively high THg concentrations were Guizhou, Guangxi, Hunan, Guangdong, Jiangxi, Shaanxi, Yunnan, Chongqing, Heilongjiang, and Hainan. These provinces, except Shaanxi and Heilongjiang, are located in South China, where double-cropping rice was planted. When we considered the provincial average rice grain THg pollution situation, we found that the average THg concentrations in all provinces were lower than the mercury limit of $20 \mu\text{g}/\text{kg}$ for Chinese rice grain⁶⁹ (Figure 3a). However, based on high-resolution rice grain THg concentrations, we determined that approximately 0.72% of grids still exceeded the rice grain THg concentrations, which were defined as heavily THg-polluted grids.

To further identify the source contributions to rice grain THg in China, we evaluated the contribution proportions of different sources to rice grain THg concentrations in different grids (Figure S9), and the probability density method was used for analysis. On average, atmospheric mercury, soil mercury, and irrigation water mercury contributed 81.3, 17.8, and 0.9%, respectively, of rice grain THg in 2017 (Figure 4a). In detail, rice leaf IHg absorption from GEM contributed the most

(73.2% on average) to the rice grain THg concentration, whereas RGM and PBM deposition and absorption by roots only accounted for 8.1%. Soil IHg and MeHg accounted for 2.5 and 15.3%, respectively, of rice grain THg. Therefore, the rice grain THg distribution characteristics were dominated by atmospheric GEM from the national perspective. However, the spatial distribution of source contribution proportions to rice grain THg significantly varied across the grid, which could be observed from the wide span of the source contribution ratio in Figure 4a. Grids with low GEM contributions were mainly located in central and southwest Guizhou (Guiyang, Anshun, and southwest Guizhou cities), Shanghai, east of Heilongjiang (Shuangyashan and Jixi), south of Jiangsu (Suzhou and Wuxi cities), and the Pearl River Delta (Foshan, Zhongshan, Zhuhai, Dongguan, and Shenzhen cities) (Figure S9). These areas, except the Pearl River Delta and Heilongjiang province, were also characterized as heavy soil mercury pollution areas with soil mercury contents that exceeded $300 \mu\text{g}/\text{kg}$ (Figure S4). The high soil contribution in the Pearl River Delta was jointly caused by relatively high soil mercury concentrations (Figure S4) and low GEM deposition (Figure S2). However, the very large difference in the soil contribution in Heilongjiang province was due to soil heterogeneity, which was mainly influenced by SOM.

3.2. Concentrations and Source Apportionment of MeHg in Rice Grain

The rice grain MeHg concentrations in China also presented a lognormal distribution with a median value of $1.30 \mu\text{g}/\text{kg}$ and varied between 0.03 and $238.5 \mu\text{g}/\text{kg}$ (Figure S8b). The provincial distribution of rice grain MeHg is shown in Figure 4b. We first ranked the provincial rice grain MeHg pollution situations according to the provincial average MeHg concentrations. The three provinces with the highest provincial average rice grain MeHg concentrations were Guizhou, Heilongjiang, and Hunan. In Guizhou province, over 89.0% of rice paddy grids had soil THg concentrations of higher than $100 \mu\text{g}/\text{kg}$. The high soil THg concentrations led to average rice grain MeHg concentrations of as high as $5.54 \mu\text{g}/\text{kg}$, which was higher than the average values for other provinces. In addition, approximately 0.27% of rice paddy grids had concentrations that exceeded $100 \mu\text{g}/\text{kg}$, and the highest value exceeded $238.6 \mu\text{g}/\text{kg}$. Heilongjiang and Hunan Provinces had heavy rice grain MeHg pollution levels of approximately 2.93 and $2.64 \mu\text{g}/\text{kg}$, respectively. However, the MeHg pollution situations differed significantly between these two provinces. The high rice grain MeHg concentrations in Hunan province were mainly due to high overall soil mercury concentrations (Figure S4), and the maximum rice grain MeHg value in Hunan was only $11.9 \mu\text{g}/\text{kg}$. However, the maximum rice grain

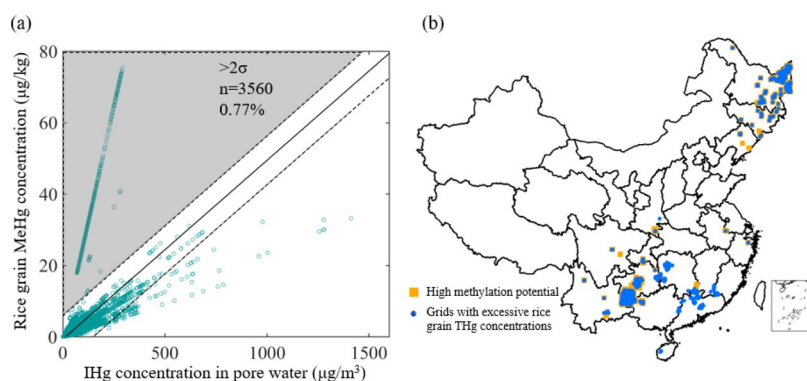


Figure 5. Methylation potential of various regions. (a) High-methylation potential area screening and (b) spatial distributions of high-methylation potential areas and grids with excessive rice grain THg concentrations (1 km × 1 km grids with a magnification factor of 50).

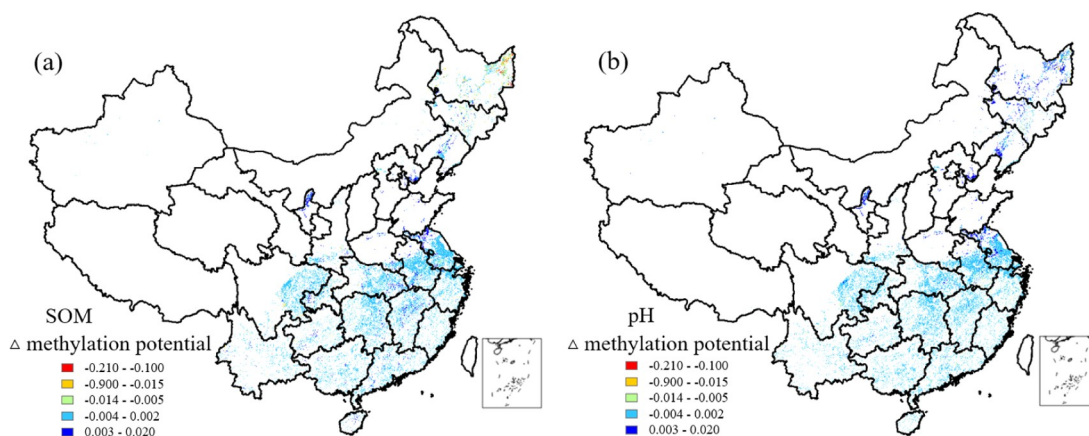


Figure 6. Methylation potential and its influencing factors (Δ methylation potential = adjusted scenario – base scenario).

MeHg concentrations in Heilongjiang province reached as high as 91.3 $\mu\text{g}/\text{kg}$, which elevated the overall provincial average values in Heilongjiang. Therefore, using the provincial average MeHg concentration to determine the rice grain MeHg pollution situations resulted in high uncertainty due to significant soil heterogeneity. This was because many grids with low rice grain MeHg concentrations offset those with high concentrations and hindered the distinction of heavily polluted regions. The existence of many singular values and the deviation between the provincial average value (black circle mask) and the median value (red line) of rice grain MeHg in most provinces indicated the importance of considering the impact of soil heterogeneity (Figure 3b).

A high-resolution rice grain MeHg distribution map would be capable of capturing heavily MeHg-polluted grids. Currently, there is no rice grain MeHg concentration limit in China. Considering the approximately 0.72% of grids with excessive rice grain THg concentrations, we determined that the top 0.72% of grids with high rice grain MeHg concentrations were heavily MeHg-polluted grids, which equaled to MeHg concentrations of higher than 11.5 $\mu\text{g}/\text{kg}$. The MeHg-polluted grids were mainly concentrated in central Guizhou province and in the junctions between Guizhou and its surrounding provinces, including Guangxi, Hunan, Chongqing, and Yunnan. Other heavily MeHg-polluted grids were sparsely distributed in southern Yunnan, southwestern Guangxi, central and southern Hunan, southeastern Fujian, northern Zhejiang, eastern Anhui, southern and southwestern Shaanxi, and eastern Heilongjiang. Compared to the

distributions of heavily THg-polluted and MeHg-polluted grids, approximately 86.4% of heavily MeHg-polluted grids were also heavily THg-polluted grids. These results indicated that although atmospheric GEM was the main source of rice grain THg nationally, the soil mercury concentration determined whether a grid exceeded the rice grain THg limit in most cases. Soil heterogeneity led to the wide span of rice grain THg concentrations across grids. However, the remaining 13.6% of the grids should also arouse our attention. Considering that MeHg is the dominant species in terms of risks to biota and human health, we need to reevaluate the necessity of determining the safety threshold of rice grain mercury based on MeHg concentrations.

In contrast to rice grain THg, MeHg in rice grains was mainly from soil mercury (64.8% on average, Figure 4b). Atmospheric mercury and irrigation water mercury accounted for 31.6 and 3.6% of rice grain MeHg, respectively. These two types of mercuries were methylated after diffusion from flood water to pore water and absorbed by rice through roots. Moreover, approximately 7.7% of the soil mercury that became rice grain MeHg was from soil IHg, and 57.1% was from soil MeHg. The soil MeHg mainly originated from in situ methylation, which indicated the significance of soil heterogeneity to the production of MeHg in the tillage layer and rice grain MeHg.

3.3. Methylation Potential of Rice Paddies

To determine the influence of soil heterogeneity on rice grain MeHg, we further analyzed the methylation potential of rice paddies across regions. The relationship between the IHg

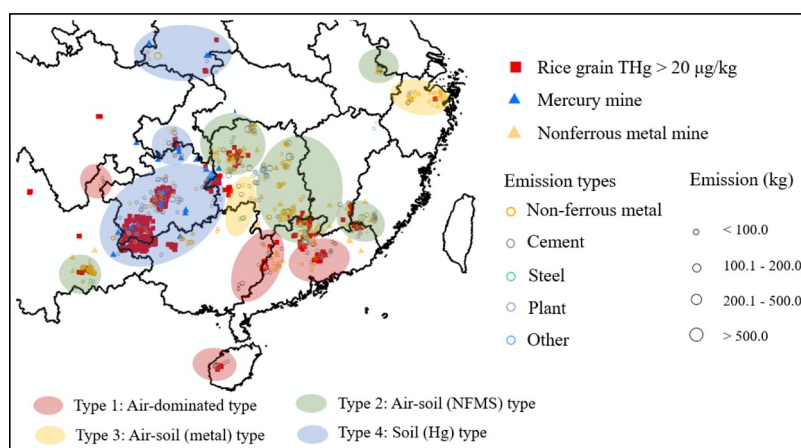


Figure 7. Rice grain THg concentrations and source types in heavily THg-polluted grids.

concentration in the pore water layer and the MeHg concentration in the rice grain (minus the contribution of soil MeHg desorption) is shown in Figure 5a. We determined the slope in Figure 5a as the methylation potential of rice paddies. Regions with greater methylation potential easily resulted in higher rice grain MeHg concentrations under similar environmental mercury concentrations. We defined the grids for which the methylation potential was over 2 standard deviations (2σ) greater than the region's mean as high-methylation potential grids, as shown in the shaded areas of the figure ($\sim 0.77\%$ of the total). Approximately, 81.2% of the grids that had high methylation potential were heavily THg-polluted (rice grain THg $> 20 \mu\text{g}/\text{kg}$, as shown in Figure 5b). We were surprised to observe that these grids were also concentrated in Guizhou province and junctions with surrounding provinces. Therefore, the extremely high rice grain MeHg concentration in Guizhou province originated from the coupled impact of high mercury input and methylation potential. Another region with high methylation potential was in Northeast China, where the production of rice grain accounted for approximately 16% of the total production in China. Therefore, although both the atmospheric mercury and soil mercury concentrations were quite low in these areas, there were still grids with heavy MeHg pollution.

To further quantify the impacts of the heterogeneity of soil components (mainly pH and SOM) on the methylation potential, we analyzed the change in the spatial distribution of the methylation potential when the values of the components were set to the national mean values for rice paddy (adjusted scenario) (Figure 6), and the base scenario was as established in Sections 2.1 and 2.2. Generally, higher SOM may provide more nutrients for methylation bacteria and, thus, promote methylation. We observed significant decreases in methylation potential in Heilongjiang and Jilin provinces, where the regional SOM was significantly higher than the national average. There were slight decreases in methylation potential in southern Guizhou, southeastern Sichuan province, and Chongqing city. The increase in pH prohibited the desorption of soil mercury, thereby reducing the methylation potential of the rice paddies. Slight decreases in the methylation potential of rice paddies were also observed in eastern Heilongjiang, central Jilin, southern Anhui, Zhejiang, southern Guizhou, western Hunan, southeastern Sichuan provinces, and Chongqing city. The combination of high SOM and low pH on average in Northeast and Southwest China jointly resulted in

high methylation potential in these two regions. In addition, we observed a much higher heterogeneity of SOM (0.16–23.7%) than pH (4.2–9.8) in rice paddies, which led to a more significant impact of SOM on the methylation potential of rice paddies.

4. IMPLICATIONS FOR POLLUTION CONTROL AND FUTURE STUDIES

Our study developed an RMTTM to identify the spatial distributions of rice grain THg and MeHg concentrations with a resolution of $1 \times 1 \text{ km}$ in China. Based on the high-resolution rice grain THg concentrations, we identified the heavily polluted THg grids with THg concentrations that exceeded the national limit of $20 \mu\text{g}/\text{kg}$ (excluding Northeast China, which is influenced by soil properties). We identified a soil mercury concentration of $520 \mu\text{g}/\text{kg}$ and a GEM deposition flux of $42 \mu\text{g}/\text{m}^2/\text{yr}$ as the criteria for judging the significance of the soil and air mercury impacts, respectively. These two values were lowest in the grids with soil mercury and GEM deposition fluxes, respectively, and highest in 0.72% of grids. We then connected the grid-specific THg to human activities and the natural geological background by comprehensively analyzing the point mercury emission inventories, historical human activities, and distribution of mineral resources.^{40,42}

Based on the grid-specific rice grain THg and source types, we divided the heavily polluted THg grids into four types, as shown in Figure 7. Type 1 was called the air-dominated type, where atmospheric mercury impact was the most significant. Grids of type 1 were mainly located in the junction between Guangxi and Guangdong provinces, central Guangdong, west of Hainan, and northeast of Yunnan. Interestingly, these grids were mainly located close to cement clinker production and nonferrous metal smelters. These two industries were generally characterized as having high emission intensity, which resulted in high deposition flux in the surrounding areas. Type 2 was called the air–soil (NFMS) type. Type 2 grids mainly corresponded to the Chang–Zhu–Tan region of Hunan, northern Huaihua of Hunan, Shaoguan city in Guangdong, Longyan city in Fujian, Honghe city in Yunnan, and Ma'anshan city in Anhui. Grids in these regions were under the coupled impact of anthropogenic mercury emissions and historical nonferrous metal melting. For example, the Chang–Zhu–Tan region was not only under the impact of current atmospheric mercury emissions but also decades of mercury

emissions and release which have led to increased mercury concentrations in the soil. Wu et al. (2014) investigated the soil mercury around a large zinc smelter in Zhuzhou city and found that over half a century of mercury emissions has led to an increase in mercury from 0.12 to 1.77 mg/kg in the soil around the smelters.⁷⁰ Type 3 was called the air–soil (metal) type. Type 3 grids were characterized by significant impacts from anthropogenic mercury emissions and historical metal mining and were mainly located in western Hunan province and northern Zhejiang province. Type 4 was called the soil (Hg) type. Rice grain MeHg in these grids was mainly related to current or historical mercury mining or the elevated geological background concentration due to surrounding mercury mines. Type 4 grids were mainly located in Guizhou and surrounding areas and in south Shaanxi province. Moreover, other highly polluted grids were mainly affected by soil properties (partial grids in Yunnan and Sichuan provinces), similar to the cause of high THg in Northeast China.

These results indicated that elevated rice grain THg pollution in China was mainly related to nonferrous metal smelters, cement clinker production, and mercury and other metal mining. For type 1 grids, it is necessary to reduce the emission intensities of related cement clinker plants and nonferrous metal smelters. If the related emission concentrations meet the standard, we need to evaluate the emission limits of nonferrous metal smelters and cement clinkers from the aspect of health protection. Alternatively, we should establish a safe distance from the sources to the agricultural land. Type 2 and type 3 grids were mainly related to historical nonferrous metal smelting or mining, which have not only led to mercury pollution but also caused other types of metal pollutions. Therefore, relevantly contaminated sites should be repaired, and multiple metals should be controlled before using them as rice paddies. For type 4 grids, which corresponded to an elevated natural geological background and mercury mining activities, soil mercury tended to be high. However, the bioavailability of mercury from geological sources was actually lower than that of mercury from anthropogenic sources. Therefore, rice grain MeHg may be overestimated in these grids. In the future, it will be necessary to distinguish the bioavailability of different sources of mercury and acquire more accurate simulation results.

Moreover, we found that the proportions of rice grain MeHg to THg varied from 1.7% to approximately 100% in China. Even within provinces, we observed a wide variation range of MeHg proportions. The resulting MeHg proportion at any given grid was reduced to a competition between atmospheric mercury absorption and soil mercury input since irrigation water mercury could be almost ignored. However, the heterogeneity of the soil was much greater than that of the atmosphere, and the soil was the main source of rice grain MeHg. This was why rice grain MeHg concentrations could be over 100 $\mu\text{g}/\text{kg}$ (Figure 2c), whereas the rice grain IHg concentration was limited to 20.1 $\mu\text{g}/\text{kg}$ (Figure S10). Therefore, soil heterogeneity dominated the significant spatial variation in the MeHg proportion. The previous assumption that rice grain MeHg concentrations respond proportionally to changes in atmospheric Hg was subject to high uncertainty.²⁶

From a global perspective, we also found that the proportion of MeHg to THg in polished rice grain varied greatly among countries or regions. Because polishing reduces the THg concentration in rice grain and has little effect on the MeHg

concentration,^{71,72} we calculated the MeHg proportion in polished rice grain by adding 10% to the simulation results according to the average increase proportion between polished rice grain and unpolished rice grain.⁷¹ As presented in Figure S11 and Table S4, the median proportion for Chinese polished rice grain from our simulation results was 32.7%, which was similar to the values in other Asian countries, with a median value of 33.5%. However, the values were significantly lower than the observed values in Europe and America. One possible explanation for this phenomenon was the high atmospheric mercury in Asia. Therefore, we can expect a quick decrease in rice grain IHg when global atmospheric mercury emissions are further reduced in the future. However, since MeHg poses a more severe health impact on human beings, the effect of mercury emission control on human health will be delayed.

Finally, there are uncertainties in the model-predicted rice grain mercury contents and source apportionment. One source of uncertainty is the sparse observational coverage of rice MeHg and large variability across regions. Second, rice grain MeHg originates mainly from soil mercury, especially in mercury-contaminated sites. Soil mercury can be traced back to anthropogenic activities that were conducted several decades ago, which have not yet been considered. Thus, the impact of atmospheric mercury emissions will be underestimated. The relationship between accumulative anthropogenic mercury emissions and release and soil mercury concentrations still requires better evaluation of the effectiveness of mercury regulatory policies. Third, due to the wide uncertainty ranges of methylation and demethylation rates, further measurements in rice paddies are needed to better constrain the model uncertainty. Fourth, the model takes into account the basic conditions of the rice field. Variables for different rice rotations and fertilizer regimes are not considered in the model, which is mainly due to the insignificant differences in mainstream measures of rice grain MeHg.^{73–75} The use of straw treatment may impact the mercury concentration and methylation process in rice fields, but due to the limited data on rice straw treatment in various regions, the effect of straw is not considered in the current model. In addition to the refinement of each parameter of rice paddies, in the future, the model can further take into account differences in management methods, straw treatment, and changes in various parameters with depth. For example, it can further distinguish diffusion or advection with depth. This will better constrain the RMTTM and provide a more accurate simulation of mercury concentrations in rice.

■ ASSOCIATED CONTENT

SI Supporting Information

The Supporting Information is available free of charge at <https://pubs.acs.org/doi/10.1021/acsenvironau.1c00061>.

Rice paddy distribution and planting regionalization; model methodology; distribution characteristics of national rice grain THg and MeHg; contributions of various sources to speciated mercury in the rice grain; rice grain IHg distribution; and regional comparison (PDF)

■ AUTHOR INFORMATION

Corresponding Author

Shuxiao Wang — State Key Joint Laboratory of Environment Simulation and Pollution Control, School of Environment,

Tsinghua University, Beijing 100084, China; State Environmental Protection Key Laboratory of Sources and Control of Air Pollution Complex, Beijing 100084, China; orcid.org/0000-0001-9727-1963; Phone: +86 1062771466; Email: shxwang@tsinghua.edu.cn; Fax: +86 1062773597

Authors

Yuying Cui – State Key Joint Laboratory of Environment Simulation and Pollution Control, School of Environment, Tsinghua University, Beijing 100084, China; State Environmental Protection Key Laboratory of Sources and Control of Air Pollution Complex, Beijing 100084, China

Qingru Wu – State Key Joint Laboratory of Environment Simulation and Pollution Control, School of Environment, Tsinghua University, Beijing 100084, China; State Environmental Protection Key Laboratory of Sources and Control of Air Pollution Complex, Beijing 100084, China; orcid.org/0000-0003-3381-4767

Kaiyun Liu – State Key Joint Laboratory of Environment Simulation and Pollution Control, School of Environment, Tsinghua University, Beijing 100084, China; State Environmental Protection Key Laboratory of Sources and Control of Air Pollution Complex, Beijing 100084, China; orcid.org/0000-0003-1659-3894

Xun Wang – State Key Laboratory of Environmental Geochemistry, Institute of Geochemistry, Chinese Academy of Sciences, Guiyang 550081, China; orcid.org/0000-0002-7407-8965

Tao Jiang – Department of Environmental Science and Engineering, Collage of Resources and Environment, Southwest University, Chongqing 400716, China

Bo Meng – State Key Laboratory of Environmental Geochemistry, Institute of Geochemistry, Chinese Academy of Sciences, Guiyang 550081, China; orcid.org/0000-0002-7827-8673

Yurong Wu – University of Chinese Academy of Sciences, Beijing 100049, China

Jia Guo – State Key Joint Laboratory of Environment Simulation and Pollution Control, School of Environment, Tsinghua University, Beijing 100084, China; State Environmental Protection Key Laboratory of Sources and Control of Air Pollution Complex, Beijing 100084, China

Complete contact information is available at: <https://pubs.acs.org/10.1021/acsenvironau.1c00061>

Author Contributions

#Y.C. and Q.W. contributed equally.

Notes

The authors declare no competing financial interest.

ACKNOWLEDGMENTS

This work was supported by the Strategic Priority Research Program of Chinese Academy of Sciences and the Pan-Third Pole Environment Study for a Green Silk Road (Pan-TPE) (XDA20040502) and the special fund of State Key Joint Laboratory of Environment Simulation and Pollution Control (22L02ESPC).

REFERENCES

- (1) Wolfe, M. F.; Schwarzbach, S.; Sulaiman, R. A. Effects of mercury on wildlife: A comprehensive review. *Environ. Toxicol. Chem.* **1998**, *17*, 146–160.
- (2) Fu, X.; Feng, X.; Sommar, J.; Wang, S. A review of studies on atmospheric mercury in China. *Sci. Total Environ.* **2012**, *421*–*422*, 73–81.
- (3) Mergler, D.; Anderson, H. A.; Chan, L. H. M.; Mahaffey, K. R.; Murray, M.; Sakamoto, M.; Stern, A. H. Methylmercury exposure and health effects in humans: A worldwide concern. *Ambio* **2007**, *36*, 3–11.
- (4) Axelrad, D. A.; Bellinger, D. C.; Ryan, L. M.; Woodruff, T. J. Dose-response relationship of prenatal mercury exposure and IQ: An integrative analysis of epidemiologic data. *Environ. Health Perspect.* **2007**, *115*, 609–615.
- (5) Roman, H. A.; Walsh, T. L.; Coull, B. A.; Dewailly, É.; Guallar, E.; Hattis, D.; Mariën, K.; Schwartz, J.; Stern, A. H.; Virtanen, J. K.; Rice, G. Evaluation of the Cardiovascular Effects of Methylmercury Exposures: Current Evidence Supports Development of a Dose-Response Function for Regulatory Benefits Analysis. *Environ. Health Perspect.* **2011**, *119*, 607–614.
- (6) Giang, A.; Selin, N. E. Benefits of mercury controls for the United States. *Proc. Natl. Acad. Sci. U.S.A.* **2016**, *113*, 286–291.
- (7) Zhang, H.; Feng, X.; Larssen, T.; Qiu, G.; Vogt, R. D. Inland China, Rice, Rather than Fish, Is the Major Pathway for Methylmercury Exposure. *Environ. Health Perspect.* **2010**, *118*, 1183–1188.
- (8) Zhang, Y.; Song, Z.; Huang, S.; Zhang, P.; Peng, Y.; Wu, P.; Gu, J.; Dutkiewicz, S.; Zhang, H.; Wu, S.; Wang, F.; Chen, L.; Wang, S.; Li, P. Global health effects of future atmospheric mercury emissions. *Nat. Commun.* **2021**, *12*, 3035.
- (9) Wang, B.; Chen, M.; Ding, L.; Zhao, Y.; Man, Y.; Feng, L.; Li, P.; Zhang, L.; Feng, X. Fish, rice, and human hair mercury concentrations and health risks in typical Hg-contaminated areas and fish-rich areas, China. *Environ. Int.* **2021**, *154*, 106561–106571.
- (10) Meng, B.; Feng, X.; Qiu, G.; Wang, D.; Liang, P.; Li, P.; Shang, L. Inorganic mercury accumulation in rice (*Oryza sativa* L.). *Environ. Toxicol. Chem.* **2012**, *31*, 2093–2098.
- (11) Zhu, Z.; Wang, X.; Wang, H.; Che-Jen, L.; Feng, X. Mercury exchange process between crop foliage and atmosphere by using single mercury isotope. *Environ. Chem.* **2018**, *37*, 419–427.
- (12) Strickman, R. J.; Mitchell, C. P. J. Accumulation and translocation of methylmercury and inorganic mercury in *Oryza sativa*: An enriched isotope tracer study. *Sci. Total Environ.* **2017**, *574*, 1415–1423.
- (13) Qin, C.; Du, B.; Yin, R.; Meng, B.; Fu, X.; Li, P.; Zhang, L.; Feng, X. Isotopic Fractionation and Source Appointment of Methylmercury and Inorganic Mercury in a Paddy Ecosystem. *Environ. Sci. Technol.* **2020**, *54*, 14334–14342.
- (14) Meng, B.; Feng, X.; Qiu, G.; Liang, P.; Li, P.; Chen, C.; Shang, L. The process of methylmercury accumulation in rice (*Oryza sativa* L.). *Environ. Sci. Technol.* **2011**, *45*, 2711–2717.
- (15) Meng, B.; Feng, X.; Qiu, G.; Cai, Y.; Wang, D.; Li, P.; Shang, L.; Sommar, J. Distribution Patterns of Inorganic Mercury and Methylmercury in Tissues of Rice (*Oryza sativa* L.) Plants and Possible Bioaccumulation Pathways. *J. Agric. Food Chem.* **2010**, *58*, 4951–4958.
- (16) Zhao, L.; Meng, B.; Feng, X. Mercury methylation in rice paddy and accumulation in rice plant: A review. *Ecotoxicol. Environ. Saf.* **2020**, *195*, 1104662–1104671.
- (17) Tang, Z.; Fan, F.; Deng, S.; Wang, D. Mercury in rice paddy fields and how does some agricultural activities affect the translocation and transformation of mercury - A critical review. *Ecotoxicol. Environ. Saf.* **2020**, *202*, 110950–110962.
- (18) Zhao, J.-Y.; Ye, Z.-H.; Zhong, H. Rice root exudates affect microbial methylmercury production in paddy soils. *Environ. Pollut.* **2018**, *242*, 1921–1929.
- (19) Rothenberg, S. E.; Feng, X. Mercury cycling in a flooded rice paddy. *J. Geophys. Res.: Biogeosci.* **2012**, *117*, 3003.

- (20) Li, Y.; Wang, Y.; Zhang, Q.; Hu, W.; Zhao, J.; Chen, Y.; Zhong, H.; Wang, G.; Zhang, Z.; Gao, Y. Elemental sulfur amendment enhance methylmercury accumulation in rice (*Oryza sativa* L.) grown in Hg mining polluted soil. *J. Hazard. Mater.* **2019**, *379*, 120701–120708.
- (21) Yin, D.; He, T.; Yin, R.; Zeng, L. Effects of soil properties on production and bioaccumulation of methylmercury in rice paddies at a mercury mining area, China. *J. Environ. Sci.* **2018**, *68*, 194–205.
- (22) Jonsson, S.; Skyllberg, U.; Nilsson, M. B.; Westlund, P.-O.; Shchukarev, A.; Lundberg, E.; Björn, E. Mercury Methylation Rates for Geochemically Relevant HgII Species in Sediments. *Environ. Sci. Technol.* **2012**, *46*, 11653–11659.
- (23) Xu, X.; Meng, B.; Zhang, C.; Feng, X.; Gu, C.; Guo, J.; Bishop, K.; Xu, Z.; Zhang, S.; Qiu, G. The local impact of a coal-fired power plant on inorganic mercury and methyl-mercury distribution in rice (*Oryza sativa* L.). *Environ. Pollut.* **2017**, *223*, 11–18.
- (24) Zhang, H.; Feng, X.; Larssen, T.; Shang, L.; Li, P. Bioaccumulation of Methylmercury versus Inorganic Mercury in Rice (*Oryza sativa* L.) Grain. *Environ. Sci. Technol.* **2010**, *44*, 4499–4504.
- (25) Liu, Y.-R.; Dong, J.-X.; Han, L.-L.; Zheng, Y.-M.; He, J.-Z. Influence of rice straw amendment on mercury methylation and nitrification in paddy soils. *Environ. Pollut.* **2016**, *209*, 53–59.
- (26) Chen, L.; Liang, S.; Liu, M.; Yi, Y.; Mi, Z.; Zhang, Y.; Li, Y.; Qi, J.; Meng, J.; Tang, X.; Zhang, H.; Tong, Y.; Zhang, W.; Wang, X.; Shu, J.; Yang, Z. Trans-provincial health impacts of atmospheric mercury emissions in China. *Nat. Commun.* **2019**, *10*, 1484.
- (27) Zhang, W.; Zhen, G.; Chen, L.; Wang, H.; Li, Y.; Ye, X.; Tong, Y.; Zhu, Y.; Wang, X. Economic evaluation of health benefits of mercury emission controls for China and the neighboring countries in East Asia. *Energy Policy* **2017**, *106*, 579–587.
- (28) Zhao, L.; Qiu, G.; Anderson, C. W. N.; Meng, B.; Wang, D.; Shang, L.; Yan, H.; Feng, X. Mercury methylation in rice paddies and its possible controlling factors in the Hg mining area, Guizhou province, Southwest China. *Environ. Pollut.* **2016**, *215*, 1–9.
- (29) Ao, M.; Xu, X.; Wu, Y.; Zhang, C.; Meng, B.; Shang, L.; Liang, L.; Qiu, R.; Wang, S.; Qian, X.; Zhao, L.; Qiu, G. Newly deposited atmospheric mercury in a simulated rice ecosystem in an active mercury mining region: High loading, accumulation, and availability. *Chemosphere* **2020**, *238*, 124630–124641.
- (30) Kwon, S. Y.; Selin, N. E.; Giang, A.; Karplus, V. J.; Zhang, D. Present and Future Mercury Concentrations in Chinese Rice: Insights From Modeling. *Global Biogeochem. Cycles* **2018**, *32*, 437–462.
- (31) Liu, Y.-R.; Johs, A.; Bi, L.; Lu, X.; Hu, H.-W.; Sun, D.; He, J.-Z.; Gu, B. Unraveling Microbial Communities Associated with Methylmercury Production in Paddy Soils. *Environ. Sci. Technol.* **2018**, *52*, 13110–13118.
- (32) Shanguan, W.; Dai, Y.; Liu, B.; Zhu, A.; Duan, Q.; Wu, L.; Ji, D.; Ye, A.; Yuan, H.; Zhang, Q.; Chen, D.; Chen, M.; Chu, J.; Dou, Y.; Guo, J.; Li, H.; Li, J.; Liang, L.; Liang, X.; Liu, H.; Liu, S.; Miao, C.; Zhang, Y. A China data set of soil properties for land surface modeling (EI). *J. Adv. Model. Earth Syst.* **2013**, *5*, 212–224.
- (33) Xu, X.; Liu, J.; Zhang, Z.; Zhou, W.; Li, R.; Yan, C.; Wu, S. X.; Shi, X. Z. Contents and development of a 5-year interval data set on spatial distribution of terrestrial ecosystems in China (1990–2010). *J. Global Change Data Detect.* **2017**, *1*, 56–63.
- (34) Liu, J.; Liu, M.; Tian, H.; Zhuang, D.; Zhang, Z.; Zhang, W.; Tang, X.; Deng, X. Spatial and temporal patterns of China's cropland during 1990–2000: An analysis based on Landsat TM data. *Remote Sens. Environ.* **2005**, *98*, 442–456.
- (35) Yang, R.; Tong, J.; Hu, B. X.; Li, J.; Wei, W. Simulating water and nitrogen loss from an irrigated paddy field under continuously flooded condition with Hydrus-1D model. *Environ. Sci. Pollut. Res.* **2017**, *24*, 15089–15106.
- (36) Lang, C.; Mao, Y.; Miao, Q. Determination of mercury in paddy water by cold vapor atomic fluorescence spectrometry. *Phys. Chem. Test. Chem* **2012**, *48*, 1240–1241.
- (37) Ao, M.; Xu, X.; Wu, Y.; Zhang, C.; Meng, B.; Shang, L.; Liang, L.; Qiu, R.; Wang, S.; Qian, X.; Zhao, L.; Qiu, G. Newly deposited atmospheric mercury in a simulated rice ecosystem in an active mercury mining region: High loading, accumulation, and availability. *Chemosphere* **2020**, *238*, 124630.
- (38) Song, Z.; Wang, C.; Ding, L.; Chen, M.; Hu, Y.; Li, P.; Zhang, L.; Feng, X. Soil mercury pollution caused by typical anthropogenic sources in China: Evidence from stable mercury isotope measurement and receptor model analysis. *J. Cleaner Prod.* **2021**, *288*, 125687–125697.
- (39) Zhou, J.; Liu, H.; Du, B.; Shang, L.; Yang, J.; Wang, Y.; International, P. R. Influence of soil mercury concentration and fraction on bioaccumulation process of inorganic mercury and methylmercury in rice (*Oryza sativa* L.). *Environ. Sci. Pollut. Res.* **2015**, *22*, 6144–6154.
- (40) Liu, K.; Wu, Q.; Wang, L.; Wang, S.; Liu, T.; Ding, D.; Tang, Y.; Li, G.; Tian, H.; Duan, L.; Wang, X.; Fu, X.; Feng, X.; Hao, J. Measure-Specific Effectiveness of Air Pollution Control on China's Atmospheric Mercury Concentration and Deposition during 2013–2017. *Environ. Sci. Technol.* **2019**, *53*, 8938–8946.
- (41) Wu, Q.; Li, G.; Wang, S.; Liu, K.; Hao, J. Mitigation Options of Atmospheric Hg Emissions in China. *Environ. Sci. Technol.* **2018**, *52*, 12368–12375.
- (42) Wu, Q.; Wang, S.; Li, G.; Liang, S.; Lin, C.-J.; Wang, Y.; Cai, S.; Liu, K.; Hao, J. Technology Temporal Trend and Spatial Distribution of Speciated Atmospheric Mercury Emissions in China During 1978–2014. *Environ. Sci. Technol.* **2016**, *50*, 13428–13435.
- (43) Wang, X.; Yuan, W.; Lin, C.-J.; Feng, X. Mercury cycling and isotopic fractionation in global forests. *Crit. Rev. Environ. Sci. Technol.* **2021**, *52*, 1–24.
- (44) Selin, N. E. Global Biogeochemical Cycling of Mercury: A Review. *Annu. Rev. Environ. Resour.* **2009**, *34*, 43–63.
- (45) Yu, X.; Driscoll, C. T.; Warby, R. A. F.; Montesdeoca, M.; Johnson, C. E. Soil mercury and its response to atmospheric mercury deposition across the northeastern United States. *Ecol. Appl.* **2014**, *24*, 812–822.
- (46) Tang, B.; Chen, J.; Wang, Z.; Qin, P.; Zhang, X. Mercury accumulation response of rice plant (*Oryza sativa* L.) to elevated atmospheric mercury and carbon dioxide. *Ecotoxicol. Environ. Saf.* **2021**, *224*, 112628–112637.
- (47) Chang, C.; Yin, R.; Huang, F.; Wang, R.; Chen, C.; Mao, K.; Feng, X.; Zhang, H. A new method of predicting the contribution of TGM to Hg in white rice: Using leaf THg and implications for Hg risk control in Wanshan Hg mine area. *Environ. Pollut.* **2021**, *288*, 117727–117734.
- (48) Yan, L.; Vogt, R.; Larssen, T. Chemistry, Environmental mercury in China: A review. *Environ. Toxicol. Chem.* **2012**, *31*, 2431–2444.
- (49) Wang, X.; Lin, C.-J.; Yuan, W.; Sommar, J.; Zhu, W.; Feng, X. Emission-dominated gas exchange of elemental mercury vapor over natural surfaces in China. *Atmos. Chem. Phys.* **2016**, *16*, 11125–11143.
- (50) Li, M.; Xi, X.; Xiao, G.; Cheng, H.; Yang, Z.; Zhou, G.; Ye, J.; Li, Z. National multi-purpose regional geochemical survey in China. *J. Geochem. Explor.* **2014**, *139*, 21–30.
- (51) Luo, H.; Cheng, Q.; Pan, X. Photochemical behaviors of mercury (Hg) species in aquatic systems: A systematic review on reaction process, mechanism, and influencing factor. *Sci. Total Environ.* **2020**, *720*, 137540–137558.
- (52) O'Driscoll, N. J.; Vost, E.; Mann, E.; Klapstein, S.; Tordon, R.; Lukeman, M.; Klapstein, S.; Robert, T.; Matthew, L. Mercury photoreduction and photooxidation in lakes: Effects of filtration and dissolved organic carbon concentration. *J. Environ. Sci.* **2018**, *68*, 151–159.
- (53) Fleck, J. A.; Gill, G.; Bergamaschi, B. A.; Kraus, T. E. C.; Downing, B. D.; Alpers, C. N. Concurrent photolytic degradation of aqueous methylmercury and dissolved organic matter. *Sci. Total Environ.* **2014**, *484*, 263–275.
- (54) Bachand, P. A. M.; Bachand, S.; Fleck, J.; Anderson, F.; Windham-Myers, L. Differentiating transpiration from evaporation in

seasonal agricultural wetlands and the link to advective fluxes in the root zone. *Sci. Total Environ.* **2014**, *484*, 232–248.

(55) Holmes, J.; Lean, D. Factors that influence methylmercury flux rates from wetland sediments. *Sci. Total Environ.* **2006**, *368*, 306–319.

(56) Gill, G. A.; Bloom, N. S.; Cappellino, S.; Driscoll, C. T.; Dobbs, C.; McShea, L.; Mason, R.; Rudd, J. W. M. Sediment–Water Fluxes of Mercury in Lavaca Bay, Texas. *Environ. Sci. Technol.* **1999**, *33*, 663–669.

(57) Tomczak, W.; Boyer, P.; Krimissa, M.; Radakovitch, O. Kd distributions in freshwater systems as a function of material type, mass-volume ratio, dissolved organic carbon and pH. *Appl. Geochem.* **2019**, *105*, 68–77.

(58) Zhao, L. *Distribution Patterns and Methylation/Demethylation Rate of Mercury in Rice Paddy in Hg Mining Area*; Southwest University, 2016.

(59) Du, S.; Wang, X.; Zhang, T.; Ding, C. Kinetic characteristics and predictive models of methylmercury production in paddy soils. *Environ. Pollut.* **2019**, *253*, 424–428.

(60) Zhao, L.; Anderson, C. W. N.; Qiu, G.; Meng, B.; Wang, D.; Feng, X. Mercury methylation in paddy soil: source and distribution of mercury species at a Hg mining area, Guizhou Province, China. *Biogeosciences* **2016**, *13*, 2429–2440.

(61) Yuan, H.; Dai, Y.; Xiao, Z.; Ji, D.; Shangguan, W. Reprocessing the MODIS Leaf Area Index products for land surface and climate modelling. *Remote Sens. Environ.* **2011**, *115*, 1171–1187.

(62) Xu, X.; Lin, Y.; Meng, B.; Feng, X.; Xu, Z.; Jiang, Y.; Zhong, W.; Hu, Y.; Qiu, G. The impact of an abandoned mercury mine on the environment in the Xiushan region, Chongqing, southwestern China. *Appl. Geochem.* **2018**, *88*, 267–275.

(63) Pang, J.; Han, J.; Fan, X.; Li, C.; Dong, X.; Liang, L.; Chen, Z. Mercury speciation, bioavailability and risk assessment on soil–rice systems from a watershed impacted by abandoned Hg mine-waste tailings. *Acta Geochim.* **2019**, *38*, 391–403.

(64) Zhao, X.; Ma, L.; Qu, P.; Yue, B.; Zhao, X.; Shang, X.; Zhao, Y.; Wu, Y. Total mercury and methylmercury in Chinese rice and dietary exposure assessment. *Food Addit. Contam., Part B* **2020**, *13*, 148–153.

(65) Zhao, H.; Yan, H.; Zhang, L.; Sun, G.; Li, P.; Feng, X. Mercury contents in rice and potential health risks across China. *Environ. Int.* **2019**, *126*, 406–412.

(66) Rothenberg, S. E.; Windham-Myers, L.; Creswell, J. E. Rice methylmercury exposure and mitigation: A comprehensive review. *Environ. Res.* **2014**, *133*, 407–423.

(67) Huang, B.; Wang, M.; Yan, L.; Sun, W.; Zhao, Y.; Shi, X.; Weindorf, D. C. Sediments, Accumulation, transfer, and environmental risk of soil mercury in a rapidly industrializing region of the Yangtze River Delta, China. *J. Soils Sediments* **2011**, *11*, 607–618.

(68) Xu, X.; Han, J.; Pang, J.; Wang, X.; Lin, Y.; Wang, Y.; Qiu, G. Methylmercury and inorganic mercury in Chinese commercial rice: Implications for overestimated human exposure and health risk. *Environ. Pollut.* **2020**, *258*, 113706–113716.

(69) *Maximum Levels of Contaminants in Foods, GB2762-2017*; National Health and Family Planning Commission of the People's Republic Of China, 2017; p 6.

(70) Wu, Q.; Wang, S.; Wang, L.; Liu, F.; Lin, C.-J.; Zhang, L.; Wang, F. Spatial distribution and accumulation of Hg in soil surrounding a Zn/Pb smelter. *Sci. Total Environ.* **2014**, *496*, 668–677.

(71) Rothenberg, S. E.; Feng, X.; Dong, B.; Shang, L.; Yin, R.; Yuan, X. Characterization of mercury species in brown and white rice (*Oryza sativa* L.) grown in water-saving paddies. *Environ. Pollut.* **2011**, *159*, 1283–1289.

(72) Rothenberg, S. E.; Mgutshini, N. L.; Bizimis, M.; Johnson-Beebout, S. E.; Ramanantsoanirina, A. Retrospective study of methylmercury and other metal(loid)s in Madagascar unpolished rice (*Oryza sativa* L.). *Environ. Pollut.* **2015**, *196*, 125–133.

(73) Sun, T.; Ma, M.; Du, H.; Wang, X.; Zhang, Y.; Wang, Y.; Wang, D. Effect of different rotation systems on mercury methylation in paddy fields. *Ecotoxicol. Environ. Saf.* **2019**, *182*, 109403–109411.

(74) Tang, Z.; Fan, F.; Wang, X.; Shi, X.; Deng, S.; Wang, D. Mercury in rice (*Oryza sativa* L.) and rice-paddy soils under long-

term fertilizer and organic amendment. *Ecotox. Environ. Saf.* **2018**, *150*, 116–122.

(75) Tang, Z.; Fan, F.; Wang, X.; Shi, X.; Wang, D. Understanding the effects of long-term different fertilizer applications on methylmercury accumulation in rice (*Oryza sativa* L.) plants. *Sci. Total Environ.* **2021**, *777*, 146125–146135.